

Robust dynamical effects in traffic and chaotic maps on trees

BOSILJKA TADIĆ* and ZORAN LEVNAJIC

Department of Theoretical Physics, Jožef Stefan Institute, Box 3000 SI-1001 Ljubljana, Slovenia

*Corresponding author. E-mail: Bosiljka.Tadic@ijs.si

Abstract. In the dynamic processes on networks collective effects emerge due to the couplings between nodes, where the network structure may play an important role. Interaction along many network links in the nonlinear dynamics may lead to a kind of chaotic collective behavior. Here we study two types of well-defined diffusive dynamics on scale-free trees: traffic of packets as navigated random walks, and chaotic standard maps coupled along the network links. We show that in both cases robust collective dynamic effects appear, which can be measured statistically and related to non-ergodicity of the dynamics on the network. Specifically, we find universal features in the fluctuations of time series and appropriately defined return-time statistics.

Keywords. Networks; traffic; chaos; return-times.

PACS Nos 05.10.-a; 64.60.aq; 89.75.Da; 05.45.Pq

1. Introduction

Discrete-time diffusion processes on complex networks are modeled by a dynamical variable attached to each node with a diffusive particle hopping among the neighboring nodes, according to a set of dynamical rules. The interaction between these dynamical variables is thus provided along the locally available network links. Hence, the network with its connectivity, clustering, possible modularity, and other hidden structural characteristics [1], may affect the course of the process and measurable statistical properties. Recently, an extensive numerical study of the navigated random walks, as models of information packets traffic on different networks [2], revealed that the structure–dynamics interrelations depend both on the network complexity and parameters of the process itself. In general, a more complex network structure leaves more room for the process adaptation and improvement of the efficiency. It has been recognized that the emergent dynamical behavior can be characterized by scale-invariant behavior with power-law distributions, in the transit times of packets $P(T_T)$, waiting times in queues $P(t_w)$, return-time statistics (autocorrelator), and correlations and fluctuations of the traffic time

series. Moreover, the same process yields sets of scaling exponents that are different for different network topologies (see recent review [2] and references therein).

Nonlinear dynamics on networks with increasing number of links may lead to a kind of chaotic collective behavior [3]. Trees are special type of graphs without loops; in a study of dynamical processes on networks, trees play a special role. For instance, a spanning tree related to the maximum dynamical flow of packets [4] contains most important paths for the process on the original graph. In another example of coupled chaotic maps on trees [5], a small tree-like subgraph 4-star appears as a dynamical motif, which captures the basic dynamical features of the whole system. Recently, the spectrum of the Laplacian operator and the return-time distribution related to the random walk on trees and locally tree-like graphs has been solved analytically [6]. The results suggest that nodes with low connectivity $q_m = 1, 2$ play a special role in the random diffusion on trees.

Here we report some new results on scale-free trees related to two types of the diffusion processes:

- navigated traffic of information packets, using model of refs [2,7];
- chaotic standard maps coupled diffusively along the tree links [5].

We focus on *non-ergodicity* of the dynamics and define and compute the appropriate statistical quantities in each process: the return-time distribution $P(\Delta t)$, and scaling of the fluctuations in time series of the dynamic variable at each node on the tree. The example of the tree with $N = 1000$ nodes that we consider is shown in figure 1. It has a node-connectivity profile with a power-law $q[i] \sim (N/i)^\gamma$, which is compatible with the degree distribution $P(q) \sim q^{-1/\gamma+1}$. In the simulations we use trees with $\gamma = 0.8$ for the traffic, and $\gamma = 0.5$ for chaotic maps dynamics. Note that in the scale-free tree a large number of nodes with minimal connectivity $q_m = 1$ occur, which are mostly attached to the hub. This number is increasing with the network size.

In §2, we describe the traffic of information packets with local search and queuing and give the results for the return-times to nodes and the noise fluctuations measured at nodes on the scale-free tree. In §3, we investigate the dynamics of coupled standard maps on the same tree and present the results for the analogous quantities, defined adequately: return-times to given phase space areas for a tree-averaged trajectory, and the time series fluctuations for each node on the tree. Section 4 contains a short summary and discussion of the results.

2. Traffic on scale-free trees

We use the model developed in refs [4,2,7,8] for transport of the information packets to the pre-specified destinations on the network, with packet navigation and queuing at nodes. The properties and the relevant parameters of the model are described in detail in ref. [2], with the numerical implementation given in ref. [8]. In short, at each time step each node creates a packet with a given rate R and sends it to a randomly selected recipient node. Each node processes a packet from top of its queue (LIFO-queue) towards one of its neighbors. The neighbor node is selected

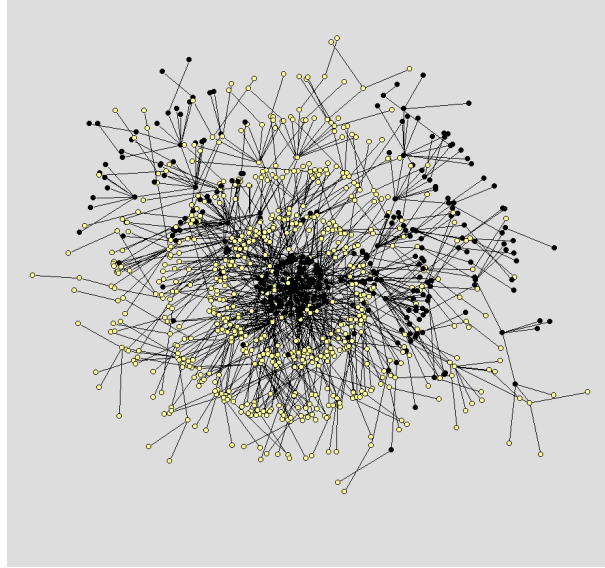


Figure 1. Scale-free tree of $N = 1000$ nodes used in the simulations. Shown are the nodes which synchronize after 10^4 steps at coupling strength $\mu = 0.011$ (pale) and unsynchronized nodes (dark).

according to mnn-navigation rule, in which the node searches for the packet's recipient address in the next-near-neighborhood. If the recipient is not in the searched area, then the packet is sent to a random neighbor, who repeats the search in its neighborhood. When the packet arrives to its destination it is removed from the network. When more than one packet is found at the same node, the packets make a queue in the buffer at that node, waiting to be processed. We use a fixed maximum buffer size $H = 1000$ packets at each node. If the buffer of a selected node is full, as at the jamming threshold, the packet cannot be delivered and waits for a further possibility to be delivered. One packet per time step is processed.

Instead of a constant creation rate R , in this work we use a constant packet density $\rho = \text{const.}$ (we typically use $\rho = 100$ packets). Each packet that arrives is in the next time step replaced by the creation of a new one, therefore assuring the constancy of ρ . In this way the stationarity of the traffic time series is guaranteed, and the limit $\rho = 1$ can be implemented precisely. This limit is important in the context of the return-time distribution (see later). In figure 2 on the top panel, we show a typical time series, representing the number nodes which are processing a packet at the same time. It was shown in refs [2,7] that such time series are fractal, with long-range correlations in the power spectrum as

$$S(f) \sim f^{-\Phi}, \quad 1 < \Phi < 2. \quad (1)$$

It was shown (see ref. [2]) that the degree of correlations in the power spectrum depends on the traffic density, in particular, it increases while approaching the jamming transition [2,9].

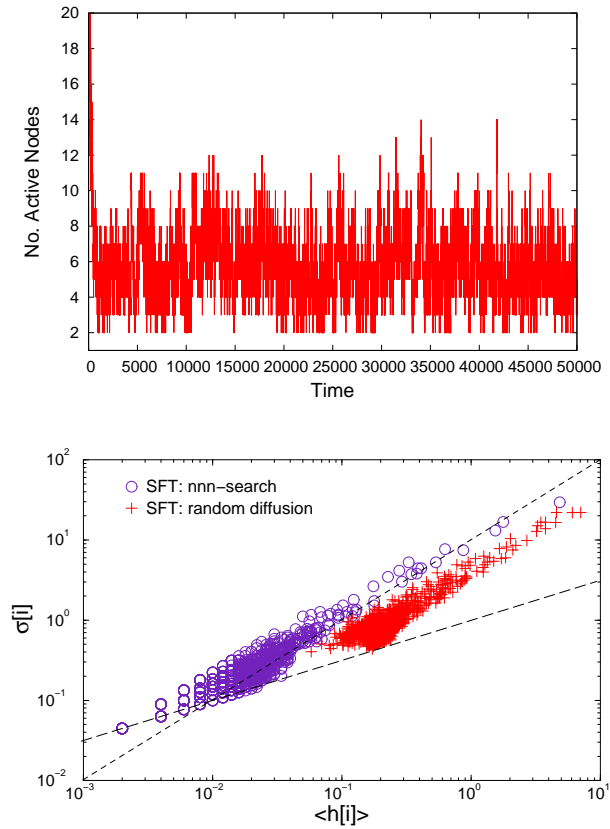


Figure 2. Top: Time series representing the number of simultaneously active nodes on the tree for packet density $\rho = 100$. Bottom: Dispersion of the time series $\{h_i(t)\}$ representing the number of packets processed by all the nodes on the tree $i = 1, 2, \dots, N$ plotted against time-average $\langle h_i(t) \rangle_t$ for a fixed posting rate $R = 10^{-3}$ and two processing algorithms.

Here we show another feature of the time series $\{h([i], t)\}$, which represents the number of packets processed by each node $i = 1, 2, \dots, N$ on the tree within a fixed time window $T_{\text{WIN}} = 10^3$ steps. In figure 2, in the bottom panel, we plot the *standard deviation* $\sigma[i]$ of the time series $h([i], t)$ against its average over many time windows $\langle h[i] \rangle_t$. Each point on the plot represents one node on the tree. The general scaling law (see ref. [10] and references therein)

$$\sigma[i] \sim \text{const.} \cdot \langle h[i] \rangle_t^\zeta, \quad (2)$$

holds. However, in contrast to non-universal slopes $1/2 < \zeta < 1$, depending on the width of time windows T_{WIN} found in networks with cycles [10], for the tree we obtained a unique exponent with a maximal value $\alpha = 1$. Furthermore, the exponent is the same for both random diffusion and nnn-navigation.

The distribution of the occupation numbers of all nodes on the tree within a given time window $T_{\text{WIN}} = 1000$ steps, shown in figure 3 (top), shows that nodes

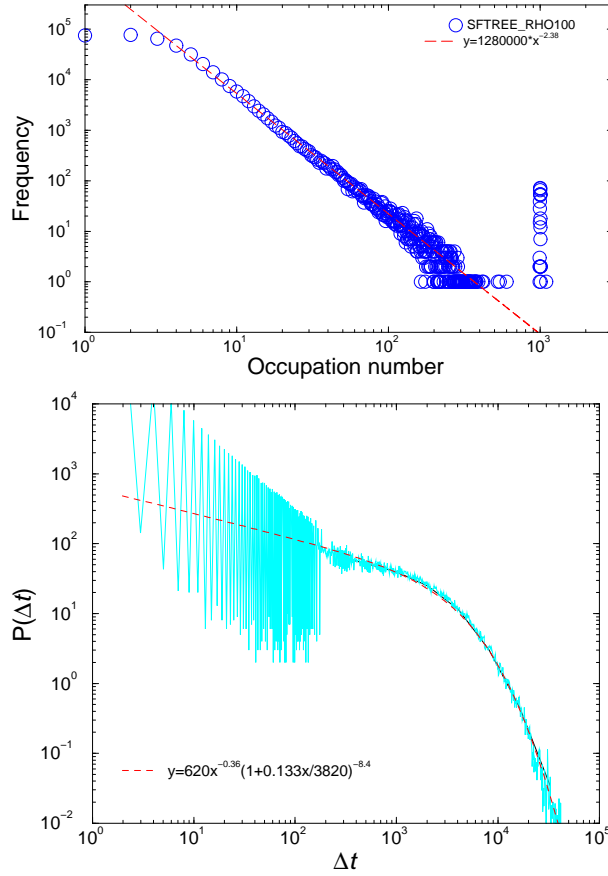


Figure 3. Top: Distribution of the occupation numbers within time window $T_{\text{WIN}} = 10^3$ of the nodes on the tree for packet density $\rho = 1000$. Bottom: Distribution of return-times Δt at a node for $\rho = 1$, averaged over all nodes and log-binned with base $b = 1.01$.

play a different role in the traffic, depending on their connectivity (number of links attached to the node). In particular, the hub is busy at each time step in correspondence to the peak at the occupation number 10^3 , whereas other nodes are gradually less involved in the process, leading to a broad distribution of the occupation numbers. The slope of the distribution follows quite closely the distribution of degree, and weakly depends on the packet density. This uneven distribution of the occupation probabilities (occupation numbers divided by T_{WIN}) is a signal of a weak ergodicity breaking [11], which occurs due to the topological inhomogeneity of the scale-free tree.

In figure 3, bottom panel, we show the simulation results for the distribution of return-times on the tree. In the general case of dense traffic, the return-time is defined as the time interval Δt between two successive events at the same node. Here we present the results in the limit $\rho = 1$, that is one packet is sent only *after*

the previous one has been delivered. In this way, Δt corresponds to the return of the walker to the origin, and then the distribution $P(\Delta t)$ corresponds to the *autocorrelator*. In ref. [6] the autocorrelator was computed analytically in the case of random walk on the infinite tree-like graphs. The power-law distribution was predicted with the scaling exponent $13/36$ [6]. In our results we fitted the numerical curve with the slope 0.36 and a (non-exponential) tail. Note that numerical results are sensitive to the finiteness of the tree also with respect to the frequency of even and odd intervals (dispersion of the curve at the lower end).

3. Coupled chaotic maps on trees

Coupled map systems (CMS) on networks are a specific class of complex systems possessing a rich variety of dynamical behavior [5,12–14] and providing models for studies of different dynamical phenomena [15–17]. Following our previous studies [5,12], we examine the collective dynamics of a system of two-dimensional Chirikov standard maps

$$\begin{pmatrix} x'[i] \\ y'[i] \end{pmatrix} = \begin{pmatrix} x[i] + y[i] + \varepsilon \sin(2\pi x[i]) \pmod{1} \\ y[i] + \varepsilon \sin(2\pi x[i]) \end{pmatrix} \quad (3)$$

coupled along the edges of a scale-free tree with $N = 1000$ nodes. The coupling is realized through the angle-coordinate (x) of the standard maps (i.e. nodes) with a fixed time delay. All the nodes are updated simultaneously according to

$$\begin{pmatrix} x[i]_{n+1} \\ y[i]_{n+1} \end{pmatrix} = (1 - \mu) \begin{pmatrix} x[i]'_n \\ y[i]'_n \end{pmatrix} + \frac{\mu}{k_i} \begin{pmatrix} \sum_{j \in \mathcal{K}_i} (x[j]_n - x[i]'_n) \\ 0 \end{pmatrix}, \quad (4)$$

where ($'$) denotes the next iterate of eq. (3), n is the global discrete time, $[i]$ indexes the tree nodes, k_i is the node degree and \mathcal{K}_i denotes the neighborhood of the node $[i]$. Therefore, the update of each node includes the values of the neighboring nodes in the previous time step. We fix the standard map chaotic parameter to $\varepsilon = 0.9$ (strong chaos) and study the dynamics of eq. (4) as a function of the network coupling strength μ . We chose the initial conditions for all the nodes randomly from the phase space subset $(x, y) \in [0, 1] \times [-1, 1]$.

For small coupling strengths up to $\mu \sim 0.02$ the dynamics of CMS eq. (4) is characterized by the inhibition of chaotic diffusion of the uncoupled standard map (eq. (3)): motion of each node takes place within a phase space band bounded in y -coordinate. Further increase of μ gives rise to the *regularization* process: after transient nodes group into certain number of clusters, with each cluster comprising the nodes that share common motion properties. Within each cluster nodes oscillate between two groups of points, firstly as a quasi-periodic orbit, and later as a periodic (regular) orbit (see ref. [18]). Also, studies of our CMS on smaller graphs (motifs) [5] revealed strange attractors as node-orbits, some of which appear to have the properties of the strange non-chaotic attractors [19]. The regularization can be quantified using the *time-averaged orbit* defined for each node $[i]$ as

$$\langle (x[i]), y[i] \rangle = \lim_{n \rightarrow \infty} \frac{1}{n - n_0} \sum_{k=n_0}^n (x[i]_k, y[i]_k), \quad (5)$$

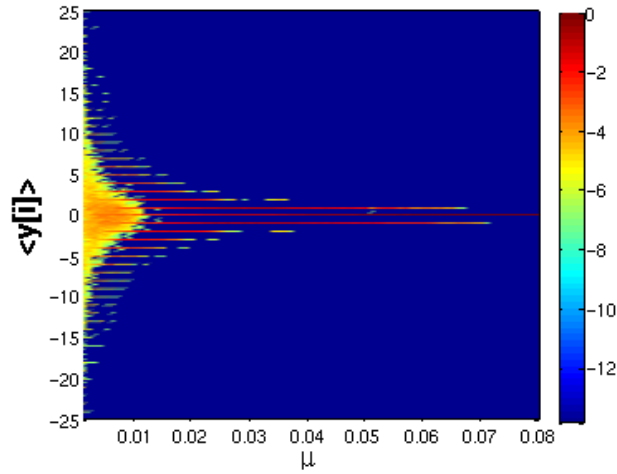


Figure 4. Regularization of nodes on the tree: two-dimensional plot of time averaged values of $\langle y[i] \rangle$ for all nodes on the tree and one set of initial conditions, plotted against coupling strength μ . Color map: number of nodes with a given $\langle y[i] \rangle$ value.

which is a phase space point that qualitatively captures the node’s motion after transient n_0 . In order to illustrate the regularity of emergent tree dynamics, in figure 4 we show a two-dimensional histogram of time-average y -coordinate $\langle y[i] \rangle$ for all the tree’s nodes, obtained for a single set of initial conditions for various μ -values. As is clear from the picture, each node at every coupling value larger than $\mu \sim 0.02$ settles to oscillate in a way to maintain a constant $\langle y[i] \rangle$. Moreover, these common values of $\langle y[i] \rangle$ (that define the clusters mentioned above) are organized as a discrete set of equally spaced values for every coupling strength. The number of different $\langle y[i] \rangle$ -values (i.e. the number of clusters) decreases with increase of μ , and eventually (for $\mu \sim 0.07$) remains with only one value $\langle y[i] \rangle = 0$ shared by all nodes.

A way to obtain a qualitative view of the tree’s overall motion is provided by the *network-averaged orbit* defined at each time step for the whole tree as

$$(\hat{x}_n, \hat{y}_n) = \frac{1}{N} \sum_{i=1}^N (x[i]_n, y[i]_n). \quad (6)$$

Network-averaged orbit gives at each time step the average phase space position of the entire network and it is useful in the study of the global CMS properties. It was employed here to study the return-time statistics of our system: we measure the distribution of the time intervals between the consecutive visits of the network-average orbit to a pre-defined region in phase space. The results are shown in figure 5: the coupled tree dynamics builds up power-law tails that follow a slope of roughly $\tau_\Delta = -2$. This slope is followed precisely in the case of coupling $\mu = 0.051$ where the tree dynamics is fully regular (cf. figure 4).

A further measure of the dynamical collective effects on the tree is given by the study of the dispersion of the time series of momentum coordinate $\{y_n[i]\}$ for all

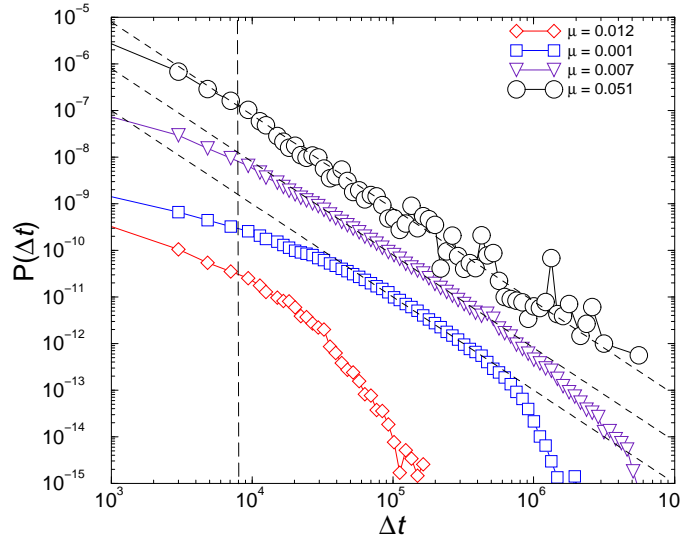


Figure 5. Distribution of the return-times to the fixed areas of the phase space in 2D coupled chaotic maps on the tree for the tree-averaged trajectory. Curves correspond to different values of the coupling μ . Slopes of dashed lines are $\tau_{\Delta} = -2$. Vertical long-dashed line marks approximate boundary of the transient regime.

the nodes, in analogy with §2 and eq. (2). In the case of chaotic CMS the time series of the value of the momentum coordinate are stochastic in the region of small couplings, where we still find the chaotic behavior, in contrast to the regular orbits. In figure 6 we report the behavior of the time series' standard deviation $\sigma[i]$ as a function of its mean value $\langle y[i] \rangle$ for all the nodes $[i]$. Again each point represents one node on the tree. Although the average values $\langle y[i] \rangle$ for all 1000 nodes span two decades, there seems to be very little variation of $\sigma[i]$ for the nodes that did not achieve regular behavior (compare figure 4 for small μ -values). If we are to compare these results with the scaling law in eq. (2), we find that the chaotic dynamics of our coupled maps is compatible with the fluctuating time series with the exponent $\zeta = 0$, in contrast to most of the 'regular' diffusion dynamics where $\zeta > 0.5$ was found. We also clearly see the process of regularization of orbits from chaotic (with large $\sigma[i]$) to regular (with small and specifically defined $\sigma[i]$). For larger μ -values (see inset) there is a precise correlation between $\sigma[i]$ and $\langle y[i] \rangle$ defining the clusters of nodes introduced previously – each cluster is specified by its $\langle y[i] \rangle$ and $\sigma[i]$ shared by the nodes of that cluster.

4. Conclusions

We studied two different types of diffusive dynamics on the scale-free trees: random-walk dynamics with local navigation and traps, and phase-coupled standard maps in their chaotic regime. We observed a variety of collective dynamical effects, arising

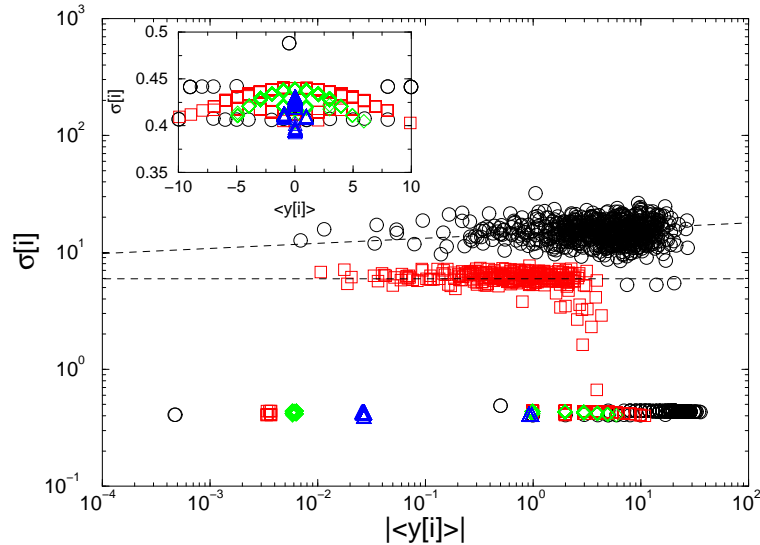


Figure 6. Dispersion of the time series $\{y_i(t)\}$ for all nodes on the tree $i = 1, 2, \dots, N$ for several values of the coupling μ . Inset: Zoom of the central area of the regular behavior on a linear scale.

due to the couplings along the tree links. In particular, we presented the results for the appropriately defined return-time distributions and fluctuations of the time series of the dynamical variables attached to network nodes in both processes.

We find several surprisingly robust scaling properties related to the tree structure. In the transport processes, the distribution of the return-times (autocorrelator) seems to be independent of both navigation and trapping of the random walks. Apart for the cut-offs, our numerical results agree with the analytical predictions for the correlator on tree-like graphs [6]. Similarly, the scaling of the time series fluctuations in the number of visits of the walker to each node exhibits a universal exponent $\zeta = 1$, both for navigated and random diffusion. The scale-free structure of the tree with the central hub node plays a crucial role in the appearance of the scaling properties and consequently in the uneven use of the phase space. On the other hand, in the case of the coupled chaotic maps on trees, the difference between nodes seem to be minimized in the chaotic phase. However, when the self-organized non-chaotic motion occurs [5] (at larger couplings) the distribution of return-times to the pre-defined areas of phase space appears to have a power-law tail with a universal scaling exponent $\tau_\Delta = -2$, away from cut-offs. In general, occurrence of a broad distribution of the return-times suggests uneven use of the phase space and non-ergodicity. We are not aware of the exact mechanisms which lead to the universal scaling exponent in this coupled dynamics.

Despite general similarities of the underlying network topology, the two considered systems show various differences in their emergent behavior which is a clear consequence of the inherently different dynamical processes being investigated. Yet, both systems display power-law tails (although with different slopes) in their statistical distributions. This represents a remarkable similarity between the two systems,

which might owe its origin to the network architecture being employed. Along with other open questions, this remains an issue for future studies.

References

- [1] S Boccaletti, V Latora, Y Moreno, M Chavez and D U Hwang, *Phys. Rep.* **424**, 175 (2006)
- [2] B Tadić, G J Rodgers and S Thurner, *Int. J. Bifurcation Chaos* **17(7)**, 2363 (2007)
- [3] D Stokic, R Hanel and S Thurner, *The window at the edge of chaos in a simple model of gene interaction networks*, *Phys. Rev. E* (2008) in press
- [4] B Tadić and S Thurner, *Physica* **A332**, 566 (2004)
- [5] Z Levnajić and B Tadić, *Self-organization in trees and motifs of two-dimensional chaotic maps with time delay*, arXiv:0711.0822v1, *J. Stat. Mech.* (2008) P03003, doi:10.1088/1742-5468/2008/03/P03003
- [6] A N Samukhin, S N Dorogovtsev and J F F Mendes, *Laplacian spectra of complex networks and random walks on them: Are scale-free architectures really important?*, arXiv:cond-mat/07061176 (2007)
- [7] B Tadić and G Rodgers, *Adv. Complex Systems* **5**, 445 (2002)
- [8] B Tadić, Modeling traffic of information packets on graphs with complex topology, in *ICCS 2003* edited by P Stoot *et al*, in *Lecture Notes in Computer Science*, Vol. 2657, pp. 136–143 (2003)
- [9] B Tadić, S Thurner and G J Rodgers, *Phys. Rev.* **E69**, 036102 (2004)
- [10] B Kujawski, B Tadić and G J Rodgers, *New J. Phys.* **9**, 154 (2007)
- [11] G Bel and E Barkai, *Europhys. Lett.* **74(1)**, 15 (2006)
- [12] Z Levnajić and B Tadić, *Lecture Notes in Computer Science* **4488**, 633 (2007)
- [13] S Jalan, R E Amritkar and C Hu, *Phys. Rev.* **E72**, 016211 (2005)
- [14] Z Jabeen and N Gupte, *Phys. Rev.* **E74**, 016210 (2006)
- [15] S Sinha and S Sinha, *Phys. Rev.* **E74**, 066117 (2006)
- [16] A Arenas, A Díaz-Guilera and C J Pérez-Vicente, *Phys. Rev. Lett.* **96**, 114102 (2006)
- [17] E G Altmann and H Kantz, *Europhys. Lett.* **78**, 10008 (2007)
- [18] Z Levnajić, Dynamical regularization in scalefree-trees of coupled 2D chaotic maps, *Lecture Notes in Computer Science Part 2*, Vol. 5102, pp. 584–592 (2008)
- [19] S S Negi and R Ramaswamy, *Pramana – J. Phys.* **56(1)**, 47 (2001)